# Coherent population oscillations and superluminal light in a protein complex

**Chandra S. Yelleswarapu, Samir Laoui, Reji Philip[1], and D. V. G. L. N. Rao[*]**

*Department of Physics, University of Massachusetts, Boston, MA, 02125, USA*
*[1]Permanent address: Raman Research Institute, Bangalore, 560080, India.*
*[*]Electronic address: raod@umb.edu*

**Abstract:** We observed superluminal light in aqueous solution of the protein complex bacteriorhodopsin (bR) at 647.1 nm wavelength where it exhibits reverse saturable behavior, exploiting the technique of coherent population oscillations (CPO). With a modulation frequency of 10 Hz, the signal pulse through a 1 cm path cell is ahead by 3 msec relative to the reference pulse, corresponding to a group velocity of -3.3 m/sec. Following our early work on slow light in the same sample at the saturable wavelength 568.2 nm, we now explicitly observed the narrow spectral hole in the absorption band of the stable B state and further, demonstrated a close correlation between the profile of the hole and the corresponding pulse delay for various modulation frequencies. A similar behavior is observed for superluminal light versus antihole blown in the absorption band.



**OCIS codes:** (190.4710) Optical nonlinearities in organic materials; (020.1670) Coherent optical effects; (160.1435) Biomaterials; (190.5530) Pulse propagation and temporal solitons.

## References and links

1. L. V. Hau, S. E. Harris, Z. Dutton, and C. H. Behroozi, "Light speed reduction to 17 meters per second in an ultracold atomic gas," Nature **397**, 594-598 (1999).
2. M. S. Bigelow, N. N. Lepeshkin, and R. W. Boyd, "Observation of ultraslow light propagation in a ruby crystal at room temperature," Phys. Rev. Lett. **90**, 1139031-1139034 (2003).
3. L. Li, X. Peng, C. Liu, H. Guo and X. Chen, "The transition time induced narrow linewidth of the electromagnetically induced transparency in cesium vapor," J. Phys. B: At. Mol. Opt. Phys. **37**, 1873-1878 (2004).
4. S. Chakrabarti, A. Pradhan, B. Ray, and P. N. Gosh, "Velocity selective optical pumping effects and electromagnetically induced transparency for D2 transitions in rubidium," J. Phys. B: At. Mol. Opt. Phys. **38**, 4321-4327 (2005).
5. S. E. Schwartz and T.Y. Tan, "Wave interactions in saturable absorbers," Appl. Phys. Lett. **10**, 4-7 (1967).
6. B. H. Soffer and B. B. McFarland, "Frequency locking and dye spectral hole burning in Q-spoiled lasers," Appl. Phys. Lett. **8**, 166-169 (1966).
7. M. Sargent III, "Spectroscopic technique based on Lamb's laser theory," Phys. Rep. **43**, 223-265 (1978).
8. L. W. Hillman, R. W. Boyd, J. Krasinski and C. R. Stroud, "Observation of a spectral hole due to population oscillations in a homogeneously broadened optical absorption line," Opt. Commun. **45**, 416-419 (1983).
9. P. Wu and D. V. G. L. N. Rao, "Controllable snail-paced light in biological bacteriorhodopsin thin film," Phys. Rev. Lett. **95**, 2536011-2536014 (2005).
10. P. C. Ku, F. Sedgwick, C. J. Chang-Hasnain, P. Palinginis, T. Li, H. Wang, S. W. Chang. and S. L. Chuang, "Slow light in semiconductor quantum wells," Opt. Lett. **29**, 2291-2293 (2004).
11. Y. Okawachi, M. Bigelow, J. Sharping, Z. Zhu, A. Schweinsberg, D. Gauthier, R. Boyd, and A. Gaeta, "Tunable all-optical delays via Brillouin slow light in an optical fiber," Phys. Rev. Lett. **94**, 1539021-1539024 (2005).
12. A. Schweinsberg, N. N. Lepeshkin, M. S. Bigelow, R. W. Boyd, and S. Jarabo, "Observation of superluminal and slow light propagation in erbium-doped optical fiber," Europhys. Lett. **73**, 218-224 (2006).
13. C. S. Yelleswarapu, R. Philip, F. J. Aranda, B. R. Kimball and D. V. G. L. N. Rao, "Slow light in bacteriorhodopsin solution using coherent population oscillations," Opt. Lett. **32**, 1788-1790 (2007).
14. M. S. Bigelow, N. N. Lepeshkin, R. W. Boyd, "Superluminal and slow light propagation in a room-temperature solid," Science **301**, 200-202 (2003).
15. V. S. Zapasskii and G. G. Kozlov, "A saturable absorber, coherent, population oscillations and slow light," Opt. Spectrosc. **100**, 419-424 (2006).
16. N. Hampp, R. Thoma, D. Oesterhelt, and C. Bräuchle, "Biological photochrome bacteriorhodopsin and its genetic variant Asp96 to Asn as media for optical pattern recognition," Appl. Opt. **31**, 1834-1841 (1992).

#90973 - $15.00 USD Received 19 Dec 2007; revised 29 Feb 2008; accepted 1 Mar 2008; published 7 Mar 2008

17. A. Foanrev, A. L. Milkaelian, B. V. Kryzhanovsky, and V. K. Salakhutdinov, "Dynamic properties of bacteriorhodopsin exposed to ultrashort light pulses," Opt. Lett. **25**, 1080-1082 (2000).
18. A. Lewis, Y. Albeck, Z. Lange, J. Benchowski, and G. Weizman, "Optical computation with negative light intensity with a plastic bacteriorhodopsin film," Science **275**, 1462-1464 (1997).
19. R. Thoma, N. Hampp, C. Brauchle, and D. Oesterhelt, "Bacteriorhodopsin films as spatial light modulators for nonlinear-optical filtering," Opt. Lett. **16**, 651-653 (1991).
20. D. V. G. L. N. Rao, F. J. Aranda, D. Narayana Rao, Z. Chen, J. A. Akkara, and M. Nakashima, "All-optical logic gates with bacteriorhodopsin films," Opt. Commun. **127**, 193-199 (1996).
21. J. D. Downie, "Real-time holographic image correction using bacteriorhodopsin," Appl. Opt. **33**, 4353-4357 (1994).
22. J. Joseph, F. J. Aranda, D. V. G. L. N. Rao, J. A. Akkara, and M. Nakashima, "Optical Fourier processing using photoinduced dichroism in a bacteriorhodopsin film," Opt. Lett. **21**, 1499-1501 (1996).
23. G. Piredda and R. W. Boyd, "Slow light by means of coherent population oscillations: laser linewidth effects," J. Eur. Opt. Soc. Rap. Pub. **2,** 070041-070044 (2007).
24. D. Gauthier and R. W. Boyd, "Fast light, slow light and optical precursors: What does it all mean?," Photonics Spectra, January, 82-90 (2007).
25. F. J. Aranda, D. V. G. L. N. Rao, C. L. Wong, P. Zhou, Z. Chen, J. A. Akkara, D. L. Kaplan and J. F. Roach, "Nonlinear optical interactions in bacteriorhodopsin using Z-scan," Opt. Rev. **2**, 204-206 (1995).

## 1. Introduction

Interaction of atomic or molecular systems with electromagnetic radiation depends on the frequency according to the Kramers-Kronig dispersion relations. The group velocity of light in the medium depends on the rate of variation of the refractive index with frequency $dn/d\omega$. When the wavelength of light corresponding to the incident pulse is tuned to the absorption band of the medium, one can achieve large dispersion and low group velocity. Such a group velocity, however, is hard to observe because light is maximally absorbed at the resonant frequency. Hence techniques such as electromagnetically induced transparency and coherent population oscillations (CPO) are employed to observe slow or superluminal light [1, 2]. Slow light is observed when $dn/d\omega$ is large and positive. On the other hand, superluminal light results when $dn/d\omega$ is large and negative. Large positive values of $dn/d\omega$ occurs in a sharp spectral hole while a large negative $dn/d\omega$ happens in a sharp spectral antihole.

In general an intense laser beam can be used to partially saturate an inhomogenously broadened absorption line, leading to the well-known Lamb dip in the absorption profile at the laser frequency [3, 4]. As the inhomogenously broadened width is much larger than the homogenous width given by dipole dephasing it is possible for spectral hole to be observed in gases at low temperatures. The possibility of such a spectral hole for homogenous broadening was theoretically studied by Schwartz and Tan [5], offering an explanation for earlier experimental observations of Soffer and McFarland [6]. In 1978, Sargent worked out detailed numerical solutions of the rate equations and demonstrated that a "coherent dip" (spectral hole) can be observed due to population pulsations in a homogenously broadened medium [7]. Such a spectral hole was experimentally observed by Hillman et al in ruby crystal with half width at half maximum of 37 Hz [8]. Recently Bigelow et al used such a spectral hole due to CPO for the demonstration of slow light in ruby at room temperature [2]. After this seminal paper, there is an explosion of research articles, and numerous researchers have demonstrated slow light in a wide variety of materials [9-13]. Even though they did not explicitly observe the spectral hole or anithole, except for a few reports [2, 12, 14], most of these experimenters successfully explained the observed pulse delays in terms of the CPO theory. On the contrary, Zapasskii et al suggest that the observed slow light effect is just a phase delay occurring in a saturable absorber [15]. Hence to establish that slow light effects genuinely originate from CPO, it is necessary to experimentally observe the profile of the spectral hole or antihole and demonstrate a correlation of the hole or anithole width with the group velocity.

To this end we carried out detailed experiments with the protein complex bacteriorhodopsin (bR) presented in this investigation. In this paper we report the experimental observation of superluminal light in bacteriorhodopsin solution at 647.1 nm where the sample exhibits reverse saturable behavior. Following our early work on slow light in bR at the saturable wavelength 568.2 nm, we now explicitly observe the narrow spectral

#90973 - $15.00 USD Received 19 Dec 2007; revised 29 Feb 2008; accepted 1 Mar 2008; published 7 Mar 2008

hole in the absorption band of the stable B state and further, demonstrate a close correlation between the profile of the hole and the corresponding pulse delay for various modulation frequencies. We also demonstrate a close correlation between the width of the antihole and pulse advancement for superluminal light.

The photo cycle of bR is shown in Fig. 1(a). In the initial *B* state of bR, called the light adapted state, the retinal chromophore is in the stable all-*trans* molecular configuration and has an absorption band at 570 nm. Upon excitation of yellow light, the chromophore undergoes light-induced isomerization. This initiates a series of structural confirmations of the bR molecule. The molecule goes through the *K*, *L* intermediate states with short lifetimes to the relatively long-lived *M* state. In the *M* state the bR molecule has *cis*-isomer configuration and has an absorption band at 410 nm. From the relatively long-lived *M* state, the molecule relaxes back to the initial *B* state through the *N*, *O* steps spontaneously. The *M* state can also revert to the initial state directly upon excitation with blue light. The photochemical stability of the films makes it possible to switch between $B \leftrightarrows M$ reversibly at relatively low power. The *M* state lifetime depends on the reprotonation process. It can be altered by different means like drying, supplying additives, reducing the temperature, and finally by genetic substitution of the aspartic acid in position 96 by asparagine (Asp96→Asn) [16]. The asparagine substitution completely inhibits the reprotonation process as a result of which the lifetime of the M sate can be substantially varied by several orders of magnitude, milliseconds to seconds. On the other hand, the M state lifetime can also be altered optically and can be made as fast as nanoseconds [17]. Due to its unique advantages, bacteriorhodopsin is one of the most suitable materials for low power nonlinear optics and several applications were demonstrated in the past in both film and solution environments [18-22]. When using light sources with wavelengths close to *B* and *M* bands, the most relevant states in the bR photocycle are the *B* and *M* isomers, because the populations of the remaining short-lived intermediate states can be neglected. Accordingly, we approximate the photoactive dynamics of bR by using a simple two-level model as shown in the Fig. 1(b).

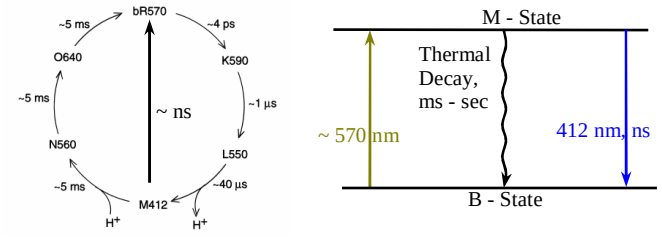


Fig. 1. bR photocycle. (a) Upon excitation with photon $h\nu_1$ the molecule goes through several short lived intermediate states to the relatively long-lived M state. The molecule goes back to the B state via thermal relaxation with lifetime of ~ 5ms or a blue photon $h\nu_2$ stimulates the photochemical relaxation to the B state. The numbers next to the letters indicate the peak absorption in nanometers. (b) Equivalent two-level model used for practical purposes.

In bR, the narrow spectral hole/antihole is created by a periodic modulation of the molecular population between *B* and *M* states. The output of Ar-Kr laser is modulated at frequency *f* using an electro-optic modulator and the resulting pulse trains contain the beating beams of the pump $Ee^{-i\omega t}$ and the probe $E_1e^{-i(\omega+\delta)t}$, where $\delta = 2\pi f$ is the detuning of the probe frequency from the pump frequency ω. The beating between the pump and probe causes the molecular population to coherently oscillate between B and M states. The oscillations lead to a rapid variation in the refractive index over a very narrow range of wavelengths which helps in modifying the group velocity. The experimental arrangement is shown in Fig. 2. The modulation depth varies with the modulation frequency from 35% at 10 Hz to 3% at 250 Hz. A beam splitter is used to sample the output of the electro-optic modulator. While the reflected beam serves as the reference arm, the transmitted beam (signal arm) goes through the 1 cm sample cell containing the bR solution. The signal and reference amplitude

#90973 - $15.00 USD Received 19 Dec 2007; revised 29 Feb 2008; accepted 1 Mar 2008; published 7 Mar 2008

modulated beams are detected using identical photodiodes and are fed to a multi-channel oscilloscope. Neutral density filters are placed in front of the detectors to ensure the signal strength is same for the same volts/division scale on the oscilloscope. Through out this paper we refer to these modulated beams as pulses and the delay between the signal and reference beams is referred to as pulse delay. Figure 3 displays the typical delay experienced for the laser wavelengths 647 nm and 570 nm. The input power is 200 mW and the spot size of the laser is 2 mm. As the laser is not focused on to the bR solution, the input intensity is 6.4 $W/cm^2$.

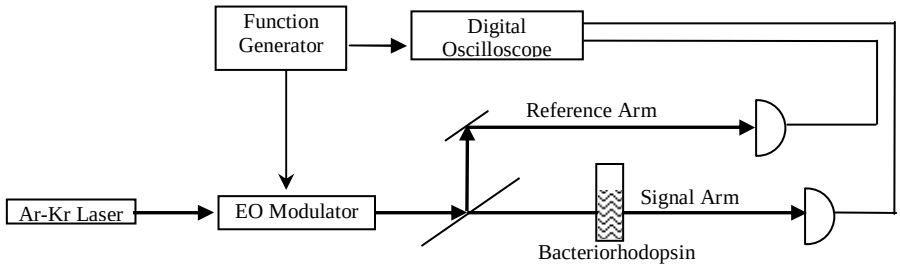


Fig. 2. Schematic of the experimental setup used for the observation of superluminal and slow light.

CPO offers several advantages over EIT in terms of generation of large group velocity variations. It works for both solids and liquids at room temperature. The pump (to saturate the transition) and probe beams are obtained from the same laser source. The laser need not be frequency stabilized and the line width can be orders of magnitude larger than the width of the spectral hole [23]. In addition, CPO in bR offers several unique advantages: it works on the flexible photoisomerization process (the lifetimes of the excited state are not fixed as in the case of electronic states in inorganic materials and can be controlled by a second independent beam), has high energy efficiency (large quantum yield for the photo reaction – ultra slow light is observed even at low light levels of microwatts), low saturation intensity, and high transparency (~100%) in operation. Both slow and superluminal light are possible in the same bR sample. A unique advantage is that not only the group index can be modified by varying the incident intensity or modulation frequency, but most significantly it can be all-optically controlled by shining an independent blue beam [9]. The possibility of all-optical switching and controllable slow and superluminal light using the same sample may offer potential applications in telecommunications such as all-optical routers.

To observe the superluminal light behavior, the periodic modulation of the population between the B and M states is obtained using the 647.1 nm output of an Ar-Kr laser. Figure 3 shows oscilloscope traces for three different scenarios: (a) with no sample in the signal arm; (b) for 647 nm input beam and (c) for 570 nm input beam. When no bR sample is in the signal arm the signal and reference pulses overlap one on top of the other as shown in Fig. 3(a). When the 1 cm sample cell containing bR solution is placed in the signal arm and the Ar-Kr laser output is tuned to 647.1 nm the signal pulse advances relative to the reference pulse as is clearly evident from the Fig. 3(b). For a modulation frequency of 25 Hz, the measured pulse width (FWHM) is ~20 msec and the pulse advancement is 1 msec. This corresponds to maximum pulse advancement (pulse advancement/FWHM) of 5%. Similarly when the laser output is 570 nm, the signal pulse delays by 3 msec (pulse width at FWHM is ~19 msec) and maximum pulse delay is 16% as shown in Fig. 3(c). Thus the signal and reference pulses are clearly separated and by varying the modulation frequency either the delay or the advancement can be changed.

#90973 - $15.00 USD Received 19 Dec 2007; revised 29 Feb 2008; accepted 1 Mar 2008; published 7 Mar 2008

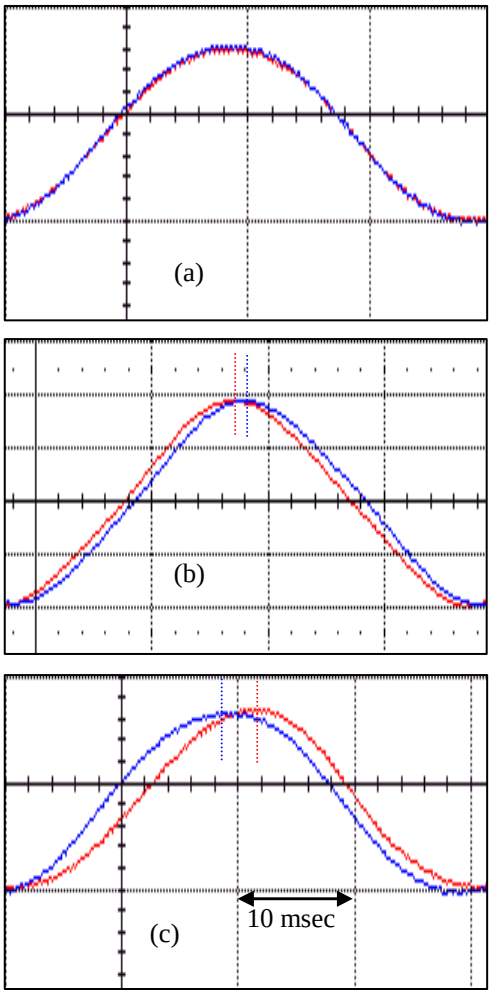


Fig. 3. Oscilloscope traces depicting the signal (red line) and reference (blue line) pulses: (a) with no sample in the signal arm, the signal and reference pulses overlap one on top of the other; (b) for 647 nm input beam and input power of 200 mW, the signal pulse advances relative to the reference pulse; (c) for 570 nm input beam and input power of 200 mW, the signal pulse is delayed relative to the reference pulse. By varying the modulation frequency either the delay or the advancement can be changed.

For the pump wavelength at 647.1 nm, we observed superluminal light at low modulation frequencies up to 40 Hz with an advancement of 3 msec at 10 Hz corresponding to a change in the group velocity of -3.33 m/sec. A gradual transition to slow light is seen as the modulation frequency is increased, as shown in Fig. 4. As the modulation frequency is varied, the modulation depth and hence the probe intensity varies. At 40 Hz, where the transition from superluminal to slow light occurs as shown in Fig. 4, we measured the modulation depth to be about 18% corresponding to a probe intensity of 1.2 W/cm$^2$. In our earlier work on z-scan at 647 nm in bR solution we reported that the sample behaves as saturable absorber for intensities below about 1.5 W/cm$^2$ and as reverse saturable absorber at higher intensities [25]. Thus the observed transition from superluminal to slow light is in line with these results.

#90973 - $15.00 USD Received 19 Dec 2007; revised 29 Feb 2008; accepted 1 Mar 2008; published 7 Mar 2008

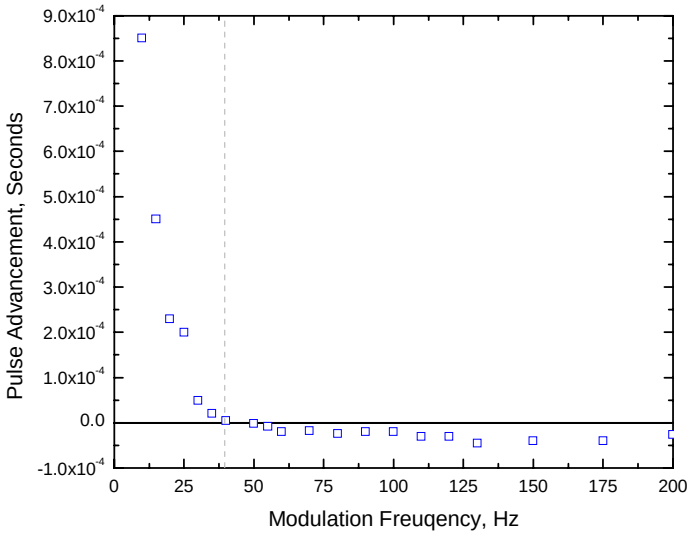


Fig. 4. Experimental observation of superluminal light for the pump wavelength of 647 nm and input power of 200 mW in bacteriorhodopsin solution of OD = 1. Dashed line represents the frequency above which the superluminal light makes gradual transition to slow light.

Figure 5 depicts the variation of the pulse advancement as the input power is changed for two modulation frequencies. The behavior of pulse advancement for superluminal light as a function of input power is similar to that of slow light pulse delay – initially the pulse advancement increases at low incident intensities and reaches a constant value at around 100 mW.

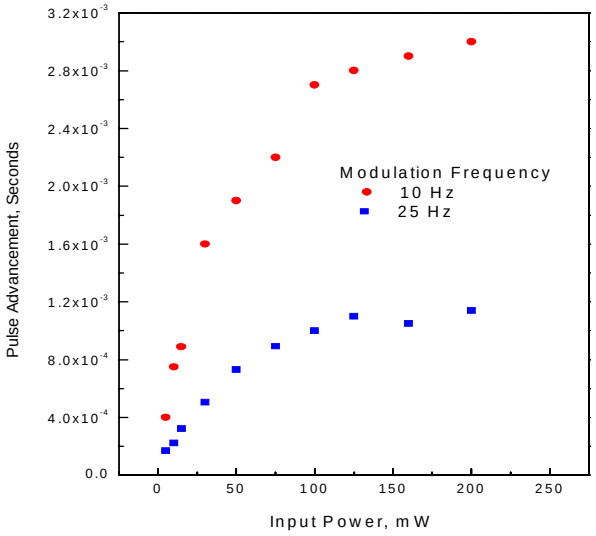


Fig. 5. Dependence of superluminal light pulse advancement with input power for modulation frequencies at 10 Hz (circles) and 25 Hz (squares).

Experimental measurements are also performed to demonstrate the creation of spectral hole and anithole in the bR solution. We measured the transmission of non-saturating probe beam in the presence of strong pump beam as the modulation frequency is varied. The pump is at frequency $\nu_1$ and probes are at sideband frequencies $\nu_2 = \nu_1 \pm f$, where $f$ is the modulation frequency. This two-mode electric field induces a polarization in the medium which in general

#90973 - $15.00 USD Received 19 Dec 2007; revised 29 Feb 2008; accepted 1 Mar 2008; published 7 Mar 2008

includes components not only at the field frequency $\nu_1$ and $\nu_2$, but also at $\nu_1 \pm k(\nu_2-\nu_1)$, where $k$ is an integer. The nonlinear pulsations (population oscillations) responding to the superposition of the modes modify the absorption coefficient resulting in a dip in the absorption profile [7]. For the bR system, the beating between the pump and probe causes the molecular population to coherently oscillate between the *B* and *M* states in the bR photocycle at the beat frequency resulting into a spectral hole. In the experiment, the outputs of the signal and reference arms are simultaneously measured for pulse delay and probe attenuation using the multi-channel oscilloscope and a lock-in amplifier. The amplitudes of the signals measured using lock-in amplifier with the sample ($I$) and without the sample ($I_0$) in the optical path are used to calculate the probe attenuation as $\ln(I_0/I)$ [5]. The experiment is performed at two wavelengths of the Ar-Kr laser – 568.2 nm and 647.1 nm – and the optical density (OD) being adjusted approximately 1 for both wavelengths. At 568.2 nm, the absorption for the *B* state of the bR is optimum whereas at 647.1 nm the absorption is small and the change in refractive index in accordance with the Kramers-Kronig dispersion relations is expected to be large.

For the pump at 647.1 nm the probe attenuation is depicted as closed squares in Fig. 6(a). A spectral antihole is observed – which is typical behavior for large and negative $dn/d\omega$. The half width at half maximum (HWHM) of the spectral antihole is about 15 Hz. Consistent with the observation in Fig. 3 – gradual transition from superluminal light to slow light at ~ 40 Hz – the probe attenuation also changes accordingly to a large and positive $dn/d\omega$, representing a spectral hole of HWHM 25 Hz. Also in Fig. 6(a), both the probe attenuation and the pulse advancement data are plotted against modulation frequency for comparison where the pulse advancement for the superluminal light regime is depicted as open squares. An interesting observation from Fig. 6(a) is that the relative variation of pulse advancement closely correlates with the variation of probe attenuation. Similarly Fig. 6(b) shows the plot of probe attenuation and pulse delay in the slow light regime (between 40 Hz to 200 Hz). In this case also the variation of the spectral hole closely correlates with the pulse delay.

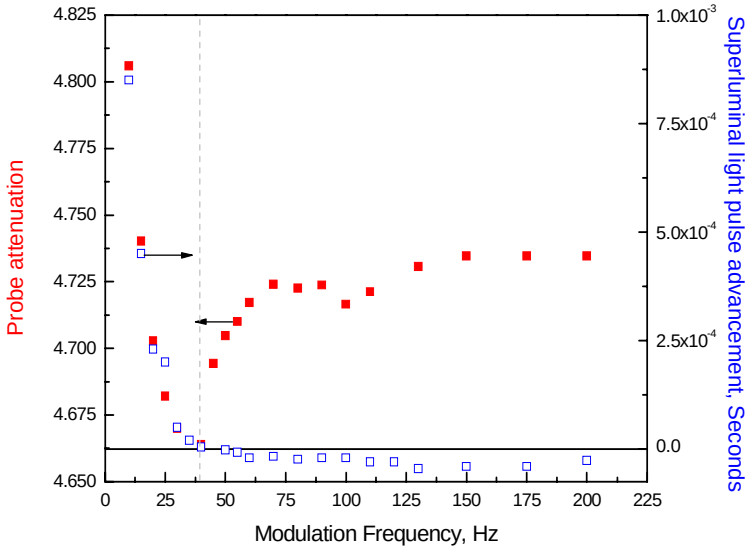


Fig. 6(a). Coherent Population oscillation in bR solution for 647.1 nm pump wavelength. The plot shows the variation of probe attenuation (closed squares) and pulse advancement (open squares) with the modulation frequency. Note that the probe attenuation and pulse advancement coincide in the superluminal light regime, up to about 40 Hz.

#90973 - $15.00 USD Received 19 Dec 2007; revised 29 Feb 2008; accepted 1 Mar 2008; published 7 Mar 2008

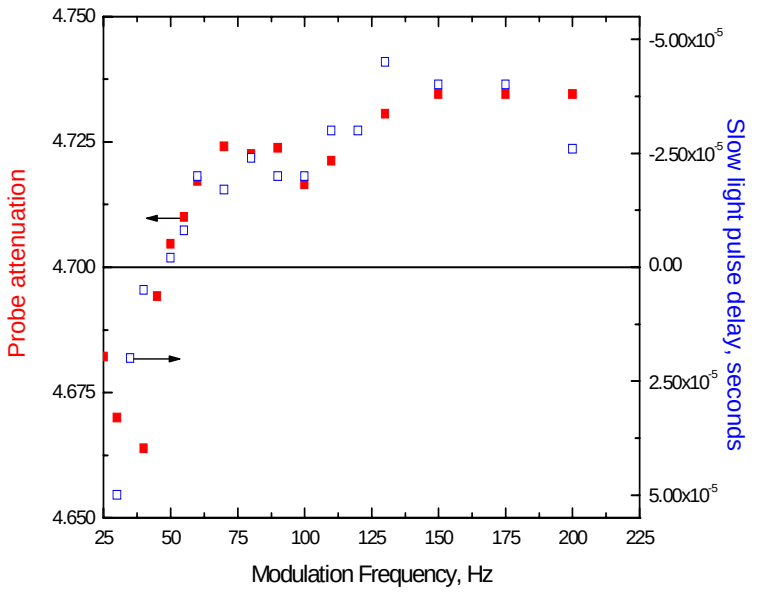


Fig. 6(b). Blowup of Fig. 6(a), plotted from 25 Hz to 225 Hz modulation frequency to show that probe attenuation (closed squares) coincides with the pulse delay (open squares) in the slow light regime also, above about 40 Hz.

For the 568.2 nm pump wavelength, the spectral hole observed agrees with our earlier reports of slow light behavior in both thin films and aqueous solution [9, 13]. Figure 7 shows the variation of probe attenuation and slow light pulse delay with the modulation frequency. For the input power of 150 mW, the HWHM of the spectral hole is ~ 50 Hz.

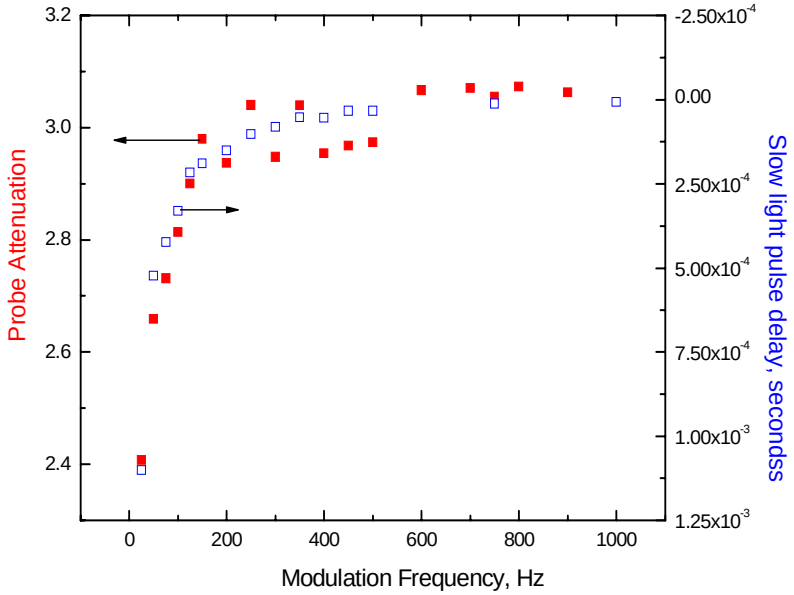


Fig. 7. CPO in bR solution for the pump at 568.2 nm. The plot shows the variation of probe attenuation (closed squares) and the slow light pulse delay (open squares) with the modulation frequency. Note that there is a close correlation between the profile of spectral hole and the associated pulse delay.

#90973 - $15.00 USD Received 19 Dec 2007; revised 29 Feb 2008; accepted 1 Mar 2008; published 7 Mar 2008

In conclusion, we have demonstrated superluminal light behavior in bacteriorhodopsin solution. Our detailed experimental observations provide convincing evidence of excellent correlation between width of the spectral hole and slow light as well as the profile of the antihole and superluminal light, indicating CPO as the mechanism of slow and fast light in the protein complex bR.

**Acknowledgment**

Thanks are due to Prof. Stephen Arnason of our Physics Department for a loan of the lock-in amplifier. This research is supported in part by a Broad Agency Announcement contract W911QY-04-C-0063 from U.S. Army Natick Soldier Center.

#90973 - $15.00 USD Received 19 Dec 2007; revised 29 Feb 2008; accepted 1 Mar 2008; published 7 Mar 2008